Supplementary Material

Progression of neuroanatomical abnormalities after first-episode of psychosis: A 3-year longitudinal sMRI study

Authors Theophilus N. Akudjedu[a,b*], Giulia Tronchin[a], Shane McInerney[a,f], Cathy Scanlon[a], Joanne P.M. Kenney[e], John McFarland[a], Gareth J. Barker[d], Peter McCarthy[c], Dara M. Cannon[a], Colm McDonald[a], Brian Hallahan[a]

Affiliations [a]Centre for Neuroimaging & Cognitive Genomics (NICOG), Clinical Neuroimaging Laboratory, NCBES Galway Neuroscience Centre, College of Medicine Nursing and Health Sciences, National University of Ireland Galway, H91TK33 Galway, Ireland. [b]Institute of Medical Imaging & Visualisation, Department of Medical Science and Public Health, Faculty of Health and Social Sciences, Bournemouth University, Bournemouth, UK.[c]Department of Radiology, College of Medicine Nursing and Health Sciences, National University of Ireland Galway, H91TK33 Galway, Ireland. [d]King's College London, Institute of Psychiatry, Psychology & Neuroscience, Department of Neuroimaging, London, UK. [e]Trinity College Institute of Neuroscience and School of Psychology, Trinity College Dublin, Dublin, Ireland. [f]Department of Psychiatry, University of Toronto, 250 College Street, 8th floor, Toronto, Canada.

Corresponding Author*

Theophilus N. Akudjedu
Institute of Medical Imaging & Visualisation,
Department of Medical Science and Public Health,
Faculty of Health and Social Sciences,
Bournemouth University,
Bournemouth, UK.
Email takudjedu@bournemouth.ac.uk

Note S1: MRI data acquisition and image pre-processing

MRI scans at both time-points were acquired at the University Hospital Galway on the same 1.5 Tesla Siemens Magnetom Symphony scanner (Erlangen, Germany), with an identical sequence at each time point. Scout sequences were used to confirm each subject's radiological positioning and image field-of-view was in alignment with the AC-PC line. A 4-channel head coil was used to acquire data, using a magnetisation-prepared rapid acquisition of gradient echo (MPRAGE) sequence to provide high resolution volumetric T1-weighted images (160 slices) with the following parameters: repetition time (TR): 1140 ms, echo time (TE): 4.38 ms, inversion time (TI): 600 ms, flip angle 15; matrix size 256 × 256; an in-plane pixel size of 0.9 mm × 0.9 mm and slice thickness of 0.9 mm. There was no major system upgrade during this research period and participants were scanned in a random order at each time point in order to minimise any acquisition bias due to any changes in scanner characteristics over time, which could otherwise potentially confound group diagnostic differences. Non-parametric non-uniform intensity normalisation (N3) was used to correct for intensity non-uniformity (Sled et al. 1998) identified in some of the structural scans after visual examination for quality as previously described (Scanlon et al. 2014).

Note S2: Longitudinal image processing

The longitudinal processing pipeline of FreeSurfer (v.5.3.0, http://surfer. nmr.mgh.harvard.edu/) (Reuter *et al.* 2012) was employed for the segmentation of subcortical structures, ventricles and to track the progression of cortical thickness changes. This pipeline operates in a semi-automated fashion, thus providing the option of checking and improving segmentation quality (Akudjedu *et al.* 2018). The technical operation of this validated analysis pipeline had been previously detailed (Reuter *et al.* 2010; Reuter and Fischl, 2011; Reuter *et al.* 2012). The images from both time points were independently analysed with the "recon-all" segmentation pipeline. Briefly, the processing steps include motion correction, removal of non-brain tissue, Talairach transformation, atlas registration as well as spherical surface mapping and segmentation. Further analysis through an inverse consistent registration (Reuter *et al.* 2010) produced a within-subject neuroanatomical space and template. The unbiased template was further reconstructed for longitudinal brain volumetry and cortical thickness change estimation after FEP within groups over time. Cortical thickness was calculated at each vertex from a specified triangulated surface as the average distance between a point on the grey/white matter boundary and the pial surface (Fischl and Dale, 2000; Han *et al.* 2006). The accuracy of this measurement approach was previously validated by direct comparison with cortical thickness measures from post-mortem brains (Rosas *et al.* 2002). For quality control, all the images were visually inspected at each of the analysis stages and segmentation/ parcellation quality improved as

deemed necessary in accordance with the FreeSurfer quality check protocols (https://surfer.nmr.mgh.harvard.edu/fswiki/QATools) using a combination of automatic and manual methods (Segonne *et al.* 2007). Given that FreeSurfer tends to overestimate hippocampal volume (Akudjedu *et al.* 2018), manually segmented hippocampal volumes were also incorporated in our analysis.

For computation of cortical thickness maps, differences between groups over time were computed from the longitudinal runs for each participant over the two time-points. Following the FreeSurfer recommendations (http://surfer.nmr.mgh.harvard.edu/) for a robust measure of cortical thickness change with increased statistical power, temporal data from each subject was then transformed into symmetrised rate of change maps using the *mris_slopes* function of the longitudinal two-stage model (Reuter *et al.* 2012) for group comparisons. The metric of symmetrised percent change (spc) per year (in % per year) reflects the total change in thickness, scaled by the interscan interval, expressed as a percentage of the average thickness (in millimetres) across the two time points. Presented mathematically as;

spc = 100 x [rate of cortical thickness change / temporal average cortical thickness] eqn (S1)

Prior to statistical analyses, all the longitudinal cortical thickness maps were smoothed using a 20-mm full width of half maximum (FWHM) Gaussian kernel to alleviate the voxel-based nature of the initial curvature and mapped to an average surface (*fsaverage*) as previously done by Zak and colleagues (2019).

Table S1: Partial correlation of regional brain volume and rate (LLOFR) changes with change in clinical and functional variables in FEP patients

Brain Region	CPZ (Time $_2$ – Time $_1$) (r, p)	PANSS (Time $_2$ – Time $_1$) (r, p)			GAF (Time $_2$ – Time $_1$) (r, p)
		Positive	Negative	General	
Caudate	0.11, 0.59	-0.14, 0.50	-0.32, 0.12	-0.18, 0.40	0.15, 0.48
Putamen	**0.49, 0.01**	0.01, 0.95	0.003, 0.99	0.06, 0.78	-0.17, 0.43
Globus pallidus	**0.44, 0.03**	-0.13, 0.55	0.06, 0.79	-0.05, 0.80	-0.08, 0.72
Nucleus Accumbens	0.09, 0.68	0.01, 0.96	0.26, 0.21	0.15, 0.47	-0.09, 0.69
Thalamus	-0.01, 0.98	-0.11, 0.61	-0.16, 0.45	-0.01, 0.98	0.21, 0.31
Hippocampus †	-0.10, 0.65	0.23, 0.27	-0.14, 0.52	0.35, 0.09	0.02, 0.94
Hippocampus ǂ	0.02, 0.94	0.36, 0.08	-0.38, 0.06	0.07, 0.75	0.02, 0.93
Amygdala	0.04, 0.85	0.02, 0.93	0.10, 0.64	-0.08, 0.71	0.33, 0.11
Total White matter	0.02, 0.92	0.003, 0.99	-0.24, 0.25	-0.32, 0.12	**0.42, 0.04**
Total Grey matter	**-0.45, 0.02**	0.05, 0.82	-0.39, 0.06	0.04, 0.87	0.32, 0.12
Third Ventricle	0.31, 0.13	-0.03, 0.87	**0.55, 0.004**	0.22, 0.30	**-0.49, 0.01**
Lateral Ventricle	0.10, 0.64	-0.17, 0.43	**0.41, 0.04**	0.14, 0.52	**-0.41, 0.04**
Left	0.07, 0.76	-0.18, 0.40	0.39, 0.06	0.13, 0.54	**-0.39, 0.05**
Right	0.14, 0.50	-0.15, 0.47	**0.43, 0.03**	0.14, 0.51	**-0.44, 0.03**
LLOFR	0.16, 0.45	-0.13, 0.53	0.13, 0.53	0.07, 0.73	-0.24, 0.24

Table S1 Legend: Change was computed as: cumulative medication dosage (CPZ equiv.) = ($Time_2$ - $Time_1$), negative symptoms = ($Time_2$ - $Time_1$), and change in global assessment of functioning scores = ($Time_2$ - $Time_1$). **Bold** = significant values; p-values presented are uncorrected; PANSS= positive and negative syndrome score (0-6 point scale); GAF= global assessment of functioning; CPZ= chlorpromazine equivalents; LLOFR = mean symmetrised % change in cortical thickness of the left lateral orbitofrontal region; † = brain volume change (Longitudinal FreeSurfer); ǂ = brain volume change (manual segmentation). Similar associations were found for both FreeSurfer and manually segmented volume changes of the hippocampus. Note: All correlations were controlled for age, gender and ICV; % volume change in brain volume = [($Time_2$ - $Time_1$)/$Time_1$)] x 100.

Table S2: Clusters showing neuroanatomical regions with different symmetrised rates of progressive cortical thickness change in FEP patients relative to HCs over time.

Cluster No.	Cluster Location*	Cluster Probability (p-value)	Number of Vertices in cluster	Cluster Size (mm^2)	Talairach coordinates of maxima		
					TalX	TalY	TalZ
Left Hemisphere							
1	Lateral orbitofrontal	<0.0001	4152	2565.55	-25.5	43.9	-9.5
2	superiorparietal	0.0107	1097	718.87	-21.9	-82.5	17.6
3	lingual	0.0114	1084	560.68	-11.3	-56.9	-2.0
4	superiortemporal	0.0199	1701	1030.02	-48.7	8.6	-23.6
5	superiorfrontal	0.0321	346	241.61	-17.7	54.5	20.7
7	banks of the superior temporal sulcus	0.0477	1640	717.70	-60.8	-33.7	3.3
8	fusiform	0.0536	846	493.23	-30.3	-59.6	-12.3
9	precuneus	0.0590	414	208.64	-19.4	-62.1	24.1
10	insula	0.0770	464	169.39	-32.5	7.5	13.2
11	rostral middle frontal	0.0785	176	116.42	-37.5	39.7	16.1
12	posterior cingulate	0.1000	326	125.24	-4.6	-11.4	38.8
13	postcentral	0.1073	97	59.22	-50.1	-17.3	35.6
14	inferiorparietal	0.1471	118	52.14	-41.4	-57.1	37.7
15	medial orbitofrontal	0.1567	177	87.25	-5.7	25.7	-23.4
Right Hemisphere							
1	superiorfrontal	0.0092	1258	648.59	7.8	-4.5	58.0
2	lateral occipital	0.0657	265	207.91	14.8	-92.3	15.7
3	middle temporal	0.0808	233	161.05	59.1	-43.0	-12.7
4	pars orbitalis	0.1318	193	152.61	35.0	39.8	-8.0
5	inferiorparietal	0.1606	39	15.64	45.3	-54.4	29.5
6	cuneus	0.1726	9	7.69	7.9	-89.4	14.5
7	paracentral	0.1806	3	1.16	12.6	-27.1	47.8
8	precentral	0.1839	3	1.19	23.9	-4.2	45.8
9	superiorparietal	0.1888	1	0.45	35.5	-46.1	52.7

Table S2 Legend: The cluster-wise p-values presented are uncorrected; * The cortical regions of the Desikan-Killiany atlas were employed

Table S3 Correlation of mean symmetrised percentage change (spc) in cortical thickness of the left lateral orbitofrontal region with the significantly changed subcortical structures and lateral ventricles in FEP patients over time

% Change in total volume	Thickness change (spc) in the LLOFR vs. change in subcortical structures and lat. ventricles		Volume change in subcortical structures vs. change in lat. ventricles	
	r	p	r	p
Caudate	0.16	0.43	**-0.52**	**0.01**
Putamen	-0.08	0.70	-0.27	0.19
Thalamus	-0.13	0.52	**-0.48**	**0.02**
Lateral ventricle	-0.07	0.72	-	-

Table S3 Legend: % volume change in each structure was computed as = [(Time $_2$ – Time $_1$)/Time $_1$)] x 100. L = left hemisphere; R = right hemisphere. Total = sum of left and right hemispheres; LLOFR = mean symmetrised % change in cortical thickness of the left lateral orbitofrontal region; **Bold** = significant values; p-values presented are uncorrected; Note: All correlations were controlled for age at baseline and gender.

Table S4: Patient subgroup comparison of progressive brain change over time

Brain Region	Baseline		Follow-up		Mean Vol. Diff. Over time (mm^3) (95% C.I)	% Vol. Diff. Over time (SE)	Group x Time		
	Adjusted Mean Vol. (mm^3) (SE)		Adjusted Mean Vol. (mm^3) (SE)				F (1,23)	p	Hedges' g
	Affective (n=12)	Non-affective (n=16)	Affective (n=12)	Non-affective (n=16)					
Caudate	7991.31 (235.20)	8232.64 (200.35)	7840.55 (218.98)	7952.84 (186.53)	127.17 (-92.87, 347.21)	2.70 (0.65)	1.14	0.30	0.42
Putamen	12516.62 (291.54)	12839.35 (248.34)	12314.58 (295.21)	12555.63 (251.47)	46.17 (-312.95, 405.29)	1.87 (0.64)	0.20	0.66	0.18
Globus pallidus	3875.34 (113.67)	3992.93 (96.83)	3873.01 (102.27)	3941.30 (87.11)	15.05 (-72.75, 102.85)	0.68 (0.87)	0.42	0.53	0.26
Nucleus accumbens	1122.52 (47.08)	1234.18 (40.10)	1128.39 (36.00)	1228.58 (30.66)	-15.09 (-107.76, 72.86)	-0.81 (2.16)	4.05	0.06	0.80
Thalamus	17066.11 (361.34)	17246.70 (307.80)	16743.72 (365.89)	16686.97 (311.67)	318.45 (-109.77, 746.67)	2.62 (0.62)	0.98	0.33	0.39
Hippocampus †	9113.37 (191.06)	8992.60 (162.75)	8982.14 (184.46)	8924.40 (157.12)	-152.50 (-193.23, 196.27)	-2.30 (1.61)	0.38	0.54	0.24
Hippocampus ǂ	5577.29 (203.00)	5642.97 (172.92)	5563.38 (193.98)	5832.28 (165.23)	-164.44 (-560.13, 231.25)	-2.29 (1.61)	0.82	0.37	0.36
Amygdala	3140.63 (79.27)	3169.90 (67.52)	3152.92 (83.13)	3249.81 (70.81)	-42.89 (-158.64, 72.86)	-1.73 (0.88)	1.07	0.31	0.41
Lateral Ventricle	18963.92 (2538.80)	17834.04 (2162.61)	19584.41 (2833.11)	19735.79 (2413.31)	-1491.37 (-3424.60, 441.86)	-7.36 (2.28)	1.41	0.25	0.47
Third Ventricle	838.50 (100.10)	976.33 (85.26)	822.22 (118.04)	1078.14 (100.55)	-114.68 (-241.14, 11.78)	-5.02 (3.12)	2.70	0.11	0.65
Total White matter	460506.42 (7362.69)	461027.56 (6271.71)	462620.53 (7641.50)	458012.06 (6509.21)	3324.14 (-10604.42, 3956.14)	0.21 (0.38)	1.87	0.18	0.54
Total Grey matter	661641.62 (7677.94)	653699.94 (6540.24)	658727.37 (8918.40)	640552.23 (7596.89)	10945.94 (-5751.15, 27643.03)	1.37 (0.60)	1.28	0.27	0.45

Table S4 Legend: Age, gender and ICV were included as covariates for all the mean adjustments and analyses; SE= standard error; C.I = confidence interval; % Vol. Diff. = percentage volume difference; calculated as follows: 100 × [(adjusted volume at follow-Up − adjusted volume at baseline)/adjusted volume at baseline] and difference between groups over time is presented; Negative value indicates a % volume decrease over time; The percent volume differences in the affective and the non-affective subgroups at baseline and follow-Up were selected to estimate the effect size (Hedges' g); **Bold** = significant values and/or large effect sizes (>0.5); p-values presented are uncorrected; † = Longitudinal FreeSurfer volumes; **ǂ =** manually segmented volumes. Of note, there was no significant difference in the results with regards to hippocampal volume deficit progression when analysis was repeated using the manual segmentation data.

Table S5: Group comparison of progressive brain change over time after removing four patients on mood stabilisers at follow-up

Brain Region	Baseline		Follow-up		Mean Vol. Diff. Over time (mm^3) (95% C.I)	% Vol. Diff. Over time (SD)	Group x Time			Group x Time x Laterality		
	Adjusted Mean Vol. (mm^3) (SE)		Adjusted Mean Vol. (mm^3) (SE)				F (1,47)	p	Hedges' g	F (1,47)	p	Hedges' g
	FEP (n=24)	HC (n=28)	FEP (n=24)	HC (n=28)								
Caudate	8066.69 (195.64)	8227.66 (180.11)	7815.28 (181.12)	8160.08 (166.74)	-168.31 (-299.57, -37.06)	-2.13 (1.51)	5.93	0.02	0.69	0.27	0.62	0.15
Putamen	12582.46 (249.30)	12428.50 (229.51)	12321.55 (242.83)	12431.64 (223.56)	-260.30 (-473.66, -46.94)	-2.08 (1.47)	5.15	0.03	0.64	0.04	0.84	0.06
Globus pallidus	3835.87 (97.22)	4010.08 (89.50)	3804.66 (92.24)	4034.37 (84.92)	-49.21 (-136.21, 37.79)	-1.26 (0.89)	2.38	0.13	0.44	0.07	0.87	0.08
Nucleus accumbens	1179.18 (33.26)	1203.81 (30.62)	1171.49 (28.22)	1207.89 (25.98)	-7.92 (-54.88, 39.04)	-0.67 (0.47)	0.55	0.46	0.21	1.03	0.30	0.29
Thalamus	16927.74 (245.80)	17729.26 (226.29)	16402.77 (236.95)	17612.87 (218.14)	-343.41 (-589.14, -97.68)	-3.51 (2.48)	9.16	0.004	0.86	0.82	0.41	0.26
Hippocampus †	8938.15 (136.02)	9197.69 (125.22)	8861.51 (140.23)	9169.06 (129.10)	-85.98 (-199.41, 27.45)	-0.98 (0.69)	2.18	0.15	0.42	0.03	0.92	0.05
Hippocampus ǂ	5541.94 (123.70)	5749.55 (113.88)	5723.21 (140.78)	5759.32 (129.61)	104.29 (-17.92, 186.49)	1.89 (1.34)	0.51	0.48	0.20	1.20	0.26	0.31
Amygdala	3187.19 (59.82)	3206.23 (55.07)	3226.30 (63.77)	3206.06 (58.71)	46.88 (-10.88,104.64)	1.48 (1.05)	1.04	0.31	0.29	3.58	0.11	0.54
Lateral Ventricle	19350.88 (1619.00)	14018.51 (1490.50)	20946.50 (1748.26)	14476.21 (1609.50)	966.82 (-39.39, 1973.03)	4.34 (3.07)	4.16	0.05	0.58	5.38	0.04	0.66
Third Ventricle	898.56 (70.16)	853.36 (64.59)	958.90 (79.91)	883.71 (73.71)	26.50 (-41.26, 94.26)	2.63 (1.86)	0.65	0.43	0.23	-	-	-
Total White matter	461846.85 (5934.91)	478050.06 (5463.87)	459239.91 (6109.57)	477764.33 (5624.66)	-667.27 (-5 222.46, 3 887.92)	-0.15 (0.11)	0.86	0.36	0.26	-	-	-
Total Grey matter	647164.33 (5216.23)	658724.29 (4802.22)	637147.48 (5486.83)	651049.26 (5051.35)	-1127.80 (-11 314.52, 9 058.92)	-0.19 (0.13)	0.19	0.67	0.12	-	-	-

Table S5 Legend: Age, gender and ICV were included as covariates for all the mean adjustments and analyses; SE= standard error; C.I = confidence interval; % Vol. Diff. = percentage volume difference; calculated as follows: 100 × [(adjusted volume at follow-Up − adjusted volume at baseline)/adjusted volume at baseline] and difference between groups over time is presented; Negative value indicates a % volume decrease over time; The percent volume differences in the affective and the non-affective subgroups at baseline and follow-Up were selected to estimate the effect size (Hedges' g); **Bold** = significant values and/or large effect sizes (>0.5); p-values presented are uncorrected; **†** = Longitudinal FreeSurfer volumes; **ǂ =** manually segmented volumes. Of note, there was no significant difference in the results with regards to hippocampal volume deficit progression when analysis was repeated using the manual segmentation data.

Fig. S1: Uncorrected *p*-value maps showing regional neuroanatomical clusters with different symmetrised rates for progressive cortical thickness change in FEP patients relative to HCs over time.

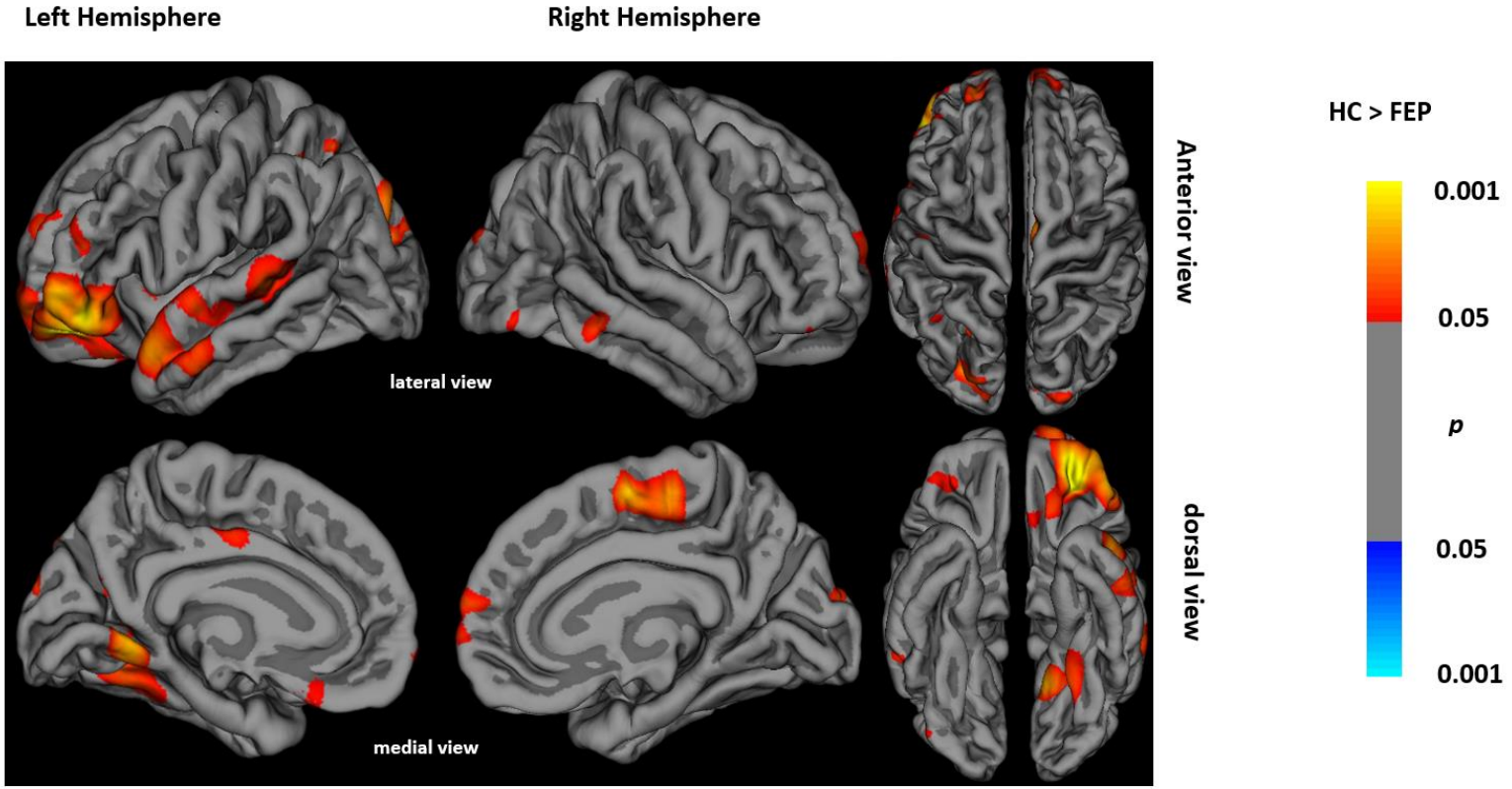

Fig. S1 Legend: The symmetrised rate of progressive cortical thickness change in FEP patients relative to healthy controls per year, mostly in the left frontal and temporal regions. Regions of cortical thinning are displayed in **RED-YELLOW** and reduced cortical thinning over time in **BLUE**

Fig. S2: Comparison of symmetrised percentage change in cortical thickness of the left lateral orbitofrontal region

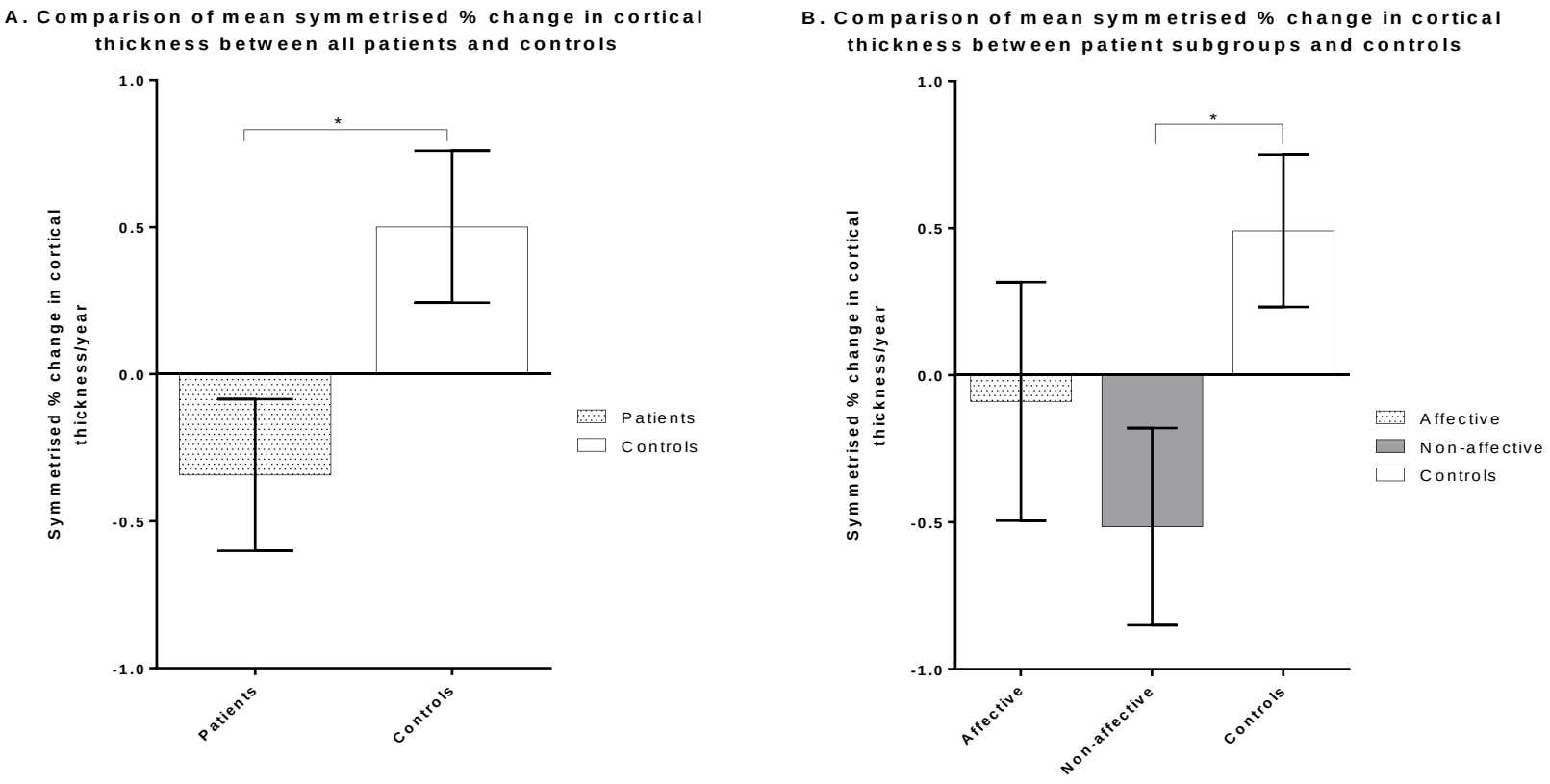

Fig. S2 Legend: Plot of corrected mean symmetrised % change (± standard error) of cortical thickness/year of the left lateral orbitofrontal region in first-episode psychosis **A.** patients (all) relative to healthy controls and **B.** patient subgroups (affective and non-affective) relative to healthy controls. The mean symmetrised % change in thickness was corrected for age at baseline and gender to describe the overall % change". Of note, the additional pairwise comparisons (affective vs. non-affective subgroups vs controls) (Fig. S2B) are presented to demonstrate the average % change in cortical thickness at the subgroup level and have not been hypothesised *a prior*. *significant difference

Fig. S3: Corrected *p*-value maps showing regional neuroanatomical clusters with increased symmetrised rates of progressive cortical thinning in FEP patients relative to HCs over time. Cluster-wise correction for multiple comparison at p=0.01.

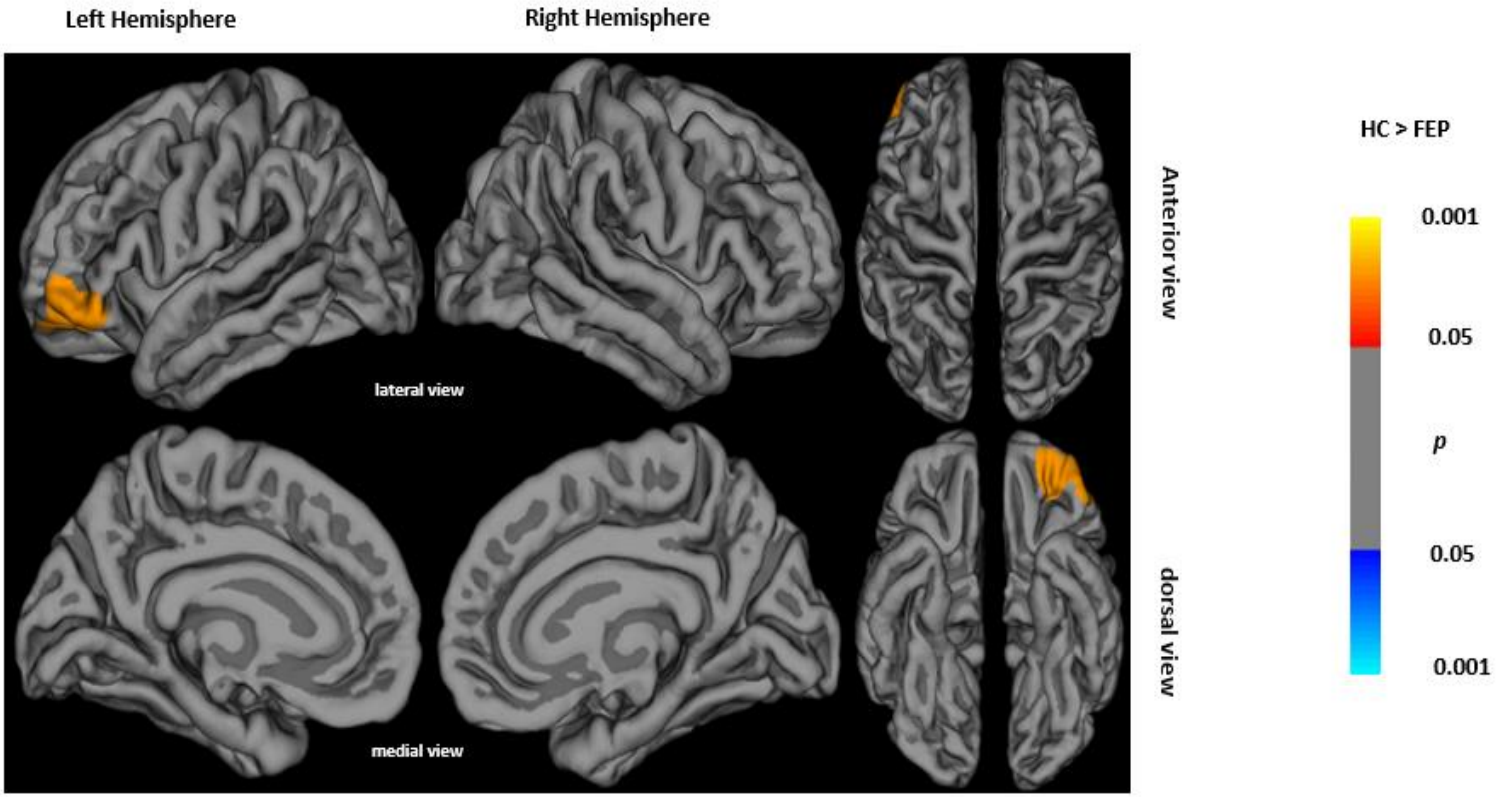

Fig. S3 Legend: The symmetrised rate of progressive cortical thickness change in FEP patients relative to healthy controls per year. The regional neuroanatomical clusters that survived cluster-wise correction for multiple comparison **(p=0.01)** for cortical thinning are displayed in **ORANGE.** This region coincides with the left lateral orbitofrontal cortex extending into aspects of the left pars orbitalis, pars triangularis, rostral middle frontal gyrus and frontal pole.

Fig. S4: Association of progressive neuroanatomical volume change with clinical variables in FEP patients

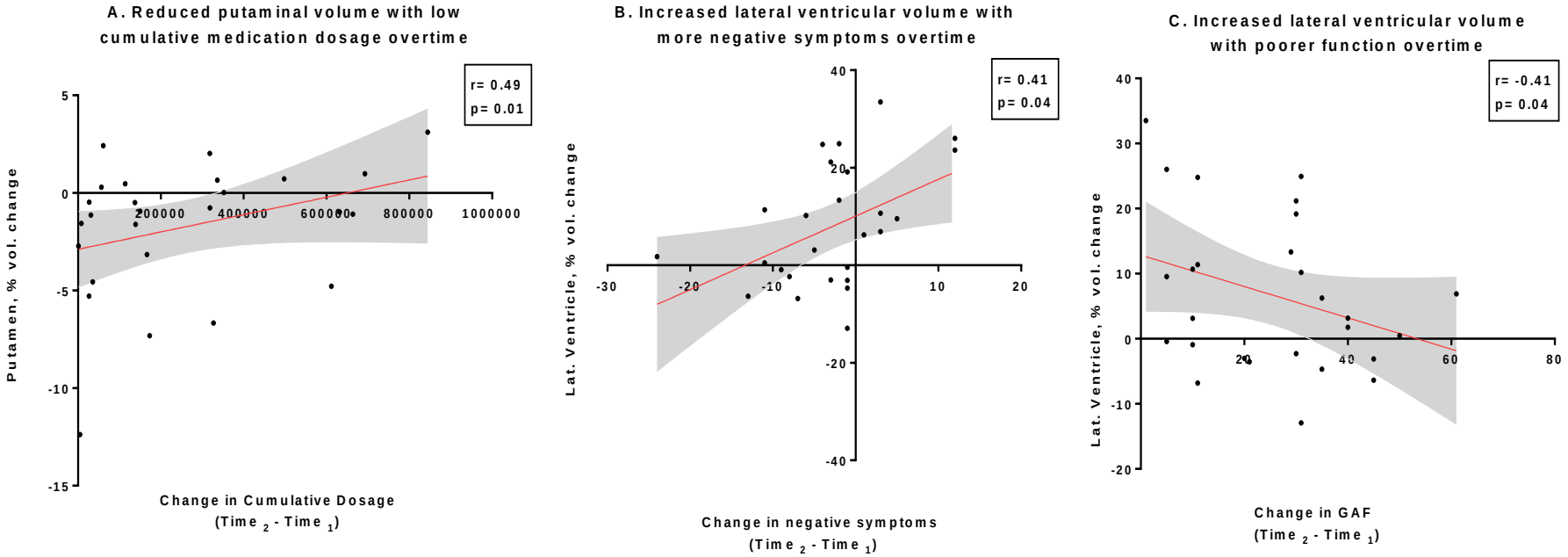

Fig. S4 Legend: A. Reduced putaminal volume associated with low cumulative medication dosage over time - change ($Time_2$ - $Time_1$) in total cumulative medication dosage (CPZ equiv.) significantly associate with % volume change in putamen. Increased lateral ventricular volume associated with: **B. Worsening negative symptoms over time -** change ($Time_2$ - $Time_1$) in negative symptoms significantly associate with % volume change in lateral ventricles. **C. Poorer global assessment of functioning over time -** change ($Time_2$ - $Time_1$) in global assessment of functioning scores significantly associate with % volume change in lateral ventricles in patients experiencing their first episode of psychosis during the 3-year period. Note: % volume change in brain volume = [($Time_2$ - $Time_1$)/$Time_1$)] x 100.

Fig. S5: Relationship between change in total volume of lateral ventricles and subcortical structures in FEP patients

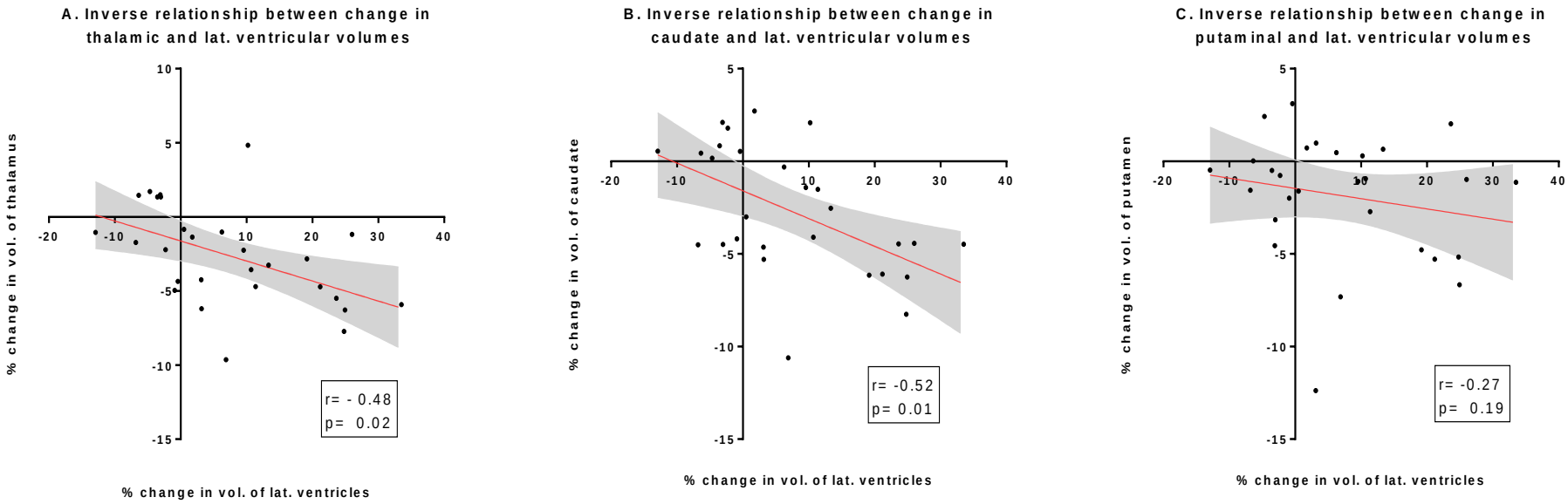

Fig. S5 Legend: A. Inverse relationship between change in lateral ventricular volume and thalamus – reduction in total thalamic volume significantly associate with enlargement in lateral ventricular volume over time. **B. Inverse relationship between change in lateral ventricular volume and caudate –** reduction in total caudate volume significantly associate with enlargement in lateral ventricular volume over time. **C. Inverse relationship between change in lateral ventricular volume and putamen –** reduction in total putamen volume significantly associate with enlargement in lateral ventricular volume over time. Note: All correlations were controlled for age, gender and ICV: % volume change in brain volume = $[(Time_2 - Time_1)/Time_1)] \times 100$.

References

1. Akudjedu, T.N., Nabulsi, L., Makelyte, M., Scanlon, C., Hehir, S., Casey, H., Ambati, S., Kenney, J., O'Donoghue, S., McDermott, E., Kilmartin, L., Dockery, P., McDonald, C., Hallahan, B., Cannon, D.M., 2018. A comparative study of segmentation techniques for the quantification of brain subcortical volume. Brain Imaging and Behavior 12(6), 1678-1695.

2. Dale, A.M., Fischl, B., Sereno, M.I., 1999. Cortical Surface-Based Analysis: I. Segmentation and Surface Reconstruction. NeuroImage 9(2), 179-194.

3. Desikan, R.S., Ségonne, F., Fischl, B., Quinn, B.T., Dickerson, B.C., Blacker, D., Buckner, R.L., Dale, A.M., Maguire, R.P., Hyman, B.T., Albert, M.S., Killiany, R.J., 2006. An automated l abelling system for subdividing the human cerebral cortex on MRI scans into gyral based regions of interest. NeuroImage 31(3), 968-980.
4. Fischl, B., Dale, A.M., 2000. Measuring the thickness of the human cerebral cortex from magnetic resonance images. Proc Natl Acad Sci U S A 97(20), 11050-11055.

5. Fischl, B., Sereno, M.I., Dale, A.M., 1999. Cortical Surface-Based Analysis: II: Inflation, Flattening, and a Surface-Based Coordinate System. NeuroImage 9(2), 195-207.

6. Han, X., Jovicich, J., Salat, D., van der Kouwe, A., Quinn, B., Czanner, S., Busa, E., Pacheco, J., Albert, M., Killiany, R., Maguire, P., Rosas, D., Makris, N., Dale, A., Dickerson, B., Fischl, B., 2006. Reliability of MRI-derived measurements of human cerebral cortical thickness: The effects of field strength, scanner upgrade and manufacturer. NeuroImage 32(1), 180-194.
7. Reuter, M., Rosas, H.D., Fischl, B., 2010. Highly accurate inverse consistent registration: A robust approach. NeuroImage 53(4), 1181-1196.

8. Reuter, M., Schmansky, N.J., Rosas, H.D., Fischl, B., 2012. Within-subject template estimation for unbiased longitudinal image analysis. NeuroImage 61(4), 1402-1418.

9. Rosas, H.D., Liu, A.K., Hersch, S., Glessner, M., Ferrante, R.J., Salat, D.H., van der Kouwe, A., Jenkins, B.G., Dale, A.M., Fischl, B., 2002. Regional and progressive thinning of the cortical ribbon in Huntington's disease. Neurology 58(5), 695-701.
10. Ségonne, F., Dale, A.M., Busa, E., Glessner, M., Salat, D., Hahn, H.K., Fischl, B., 2004. A hybrid approach to the skull stripping problem in MRI. NeuroImage 22(3), 1060-1075.

11. Segonne, F., Pacheco, J., Fischl, B., 2007. Geometrically Accurate Topology-Correction of Cortical Surfaces Using Nonseparating Loops. IEEE Transactions on Medical Imaging 26(4), 518-529.

12. Zak, N., Bøen, E., Boye, B., Andreassen, O.A., Doan, N.T., Malt, U.F., Westlye, L.T., Elvsåshagen, T., 2019. Mood episodes are associated with increased cortical thinning: A longitudinal study of bipolar disorder type II. Bipolar Disorders 0(0).